

# $\gamma$ -rays from molecular clouds illuminated by accumulated diffusive protons. II: interacting supernova remnants

Hui Li<sup>1</sup> and Yang Chen<sup>1,2\*</sup>

<sup>1</sup>*Department of Astronomy, Nanjing University, Nanjing 210093, P. R. China*

<sup>2</sup>*Key Laboratory of Modern Astronomy and Astrophysics, Nanjing University, Ministry of Education, Nanjing 210093, China*

## ABSTRACT

Recent observations reveal that spectral breaks at  $\sim$ GeV are commonly present in Galactic  $\gamma$ -ray supernova remnants (SNRs) interacting with molecular clouds and that most of them have a spectral ( $E^2 dF/dE$ ) “platform” extended from the break to lower energies. In paper I (Li & Chen 2010), we developed an accumulative diffusion model by considering an accumulation of the diffusive protons escaping from the shock front throughout the history of the SNR expansion. In this paper, we improve the model by incorporating finite-volume of MCs, demonstrate the model dependence on particle diffusion parameters and cloud size, and apply it to nine interacting SNRs (W28, W41, W44, W49B, W51C, Cygnus Loop, IC443, CTB 37A, and G349.7+0.2). This refined model naturally explains the GeV spectral breaks and, especially, the “platform”s, together with available TeV data. We find that the index of the diffusion coefficient  $\delta$  is in the range of 0.5–0.7, similar to the galactic averaged value, and the diffusion coefficient for cosmic rays around the SNRs is essentially two orders of magnitude lower than the Galactic average ( $\chi \sim 0.01$ ), which is a good indication for the suppression of cosmic ray diffusion near SNRs.

**Key words:** ISM: supernova remnants

## 1 INTRODUCTION

Supernova remnants (SNRs) are commonly believed to be one of the most important acceleration sites for the cosmic rays (CRs) below the “knee” in our Galaxy. Diffusive shock acceleration (DSA) is the prevailing acceleration mechanism, which can naturally gain a power-law population of relativistic electrons/protons (Blandford & Eichler 1987). Although multi-wavelength analysis has been intensively made for the emission of SNRs, it is still in hot debate whether the  $\gamma$ -rays from them are of hadronic or leptonic origin. Recently,  $\gamma$ -ray telescopes of new generation, such as *Fermi*-LAT and H.E.S.S., provided more and more clues that SNRs interacting with molecular clouds (MCs) may emit  $\gamma$ -rays arisen from  $\pi^0$  decay via proton-proton collision (e.g., Abdo et al. 2009, 2010a,b,c,d; Aharonian et al. 2008a,b).

Interacting SNRs, distinguished by several kinds of evidence such as OH masers, molecular line broadening, etc. (see Jiang et al. 2009 and references therein), represent a promising class of  $\gamma$ -ray sources. It is seen that some of the SNRs exhibit a spectral break at  $\sim$ GeV, such as W28, W44, W51C, IC443, etc. Most of them have a spectral ( $E^2 dF/dE$ ) “platform” extended from the break to low energies. By coin-

cidence, the  $\gamma$ -ray emitting SNRs which harbor OH masers (Hewitt et al. 2009) all have GeV breaks. The spectral break can be explained in the hadronic scenario either by different acceleration effects in the SNR-MC system, such as Alfvén wave evanescence in the weakly ionized dense gas (Malkov, Diamond & Sagdeev 2010), reacceleration model for crushed clouds (Uchiyama et al. 2010), and two-step acceleration model in the reflected shocks (Inoue, Yamazaki & Inutsuka 2010), time-dependent two-zone model (Tang et al. 2011), or by diffusion effects of CRs escaping from SNR shock (Li & Chen 2010, hereafter Paper I; Ohira, Murase, & Yamazaki 2011).

In Paper I, we developed an accumulative diffusion model by considering the accumulation of the diffusive protons escaping from the shock front throughout the history of the SNR expansion; the power-law distribution is assumed for the escaping protons and the spectrum of the diffusive protons at any point near the SNR is obtained. This model is used to explain the GeV break and GeV/TeV flux discrepancy for the four sources around SNR W28. Comparing with the point source injection (Aharonian & Atoyan 1996; Gabici et al. 2009), our model is more physical when applied to the finite-size accelerator, such as SNRs, and small

\* E-mail: ygchen@nju.edu.cn

distance between the accelerator and MC is allowed.<sup>1</sup> Almost meantime, Ohira et al. (2011) have also developed a diffusion model by considering finite-size MCs interacted by the CRs escaping from the SNRs which are imbedded in MCs and used the model to fit the  $\gamma$ -ray spectra of four SNRs (W28, W44, W51C, and IC443). In their model, the time evolution of maximum particle energy is considered and mono-momentum is assumed for the escaping particles and the spectral shape of the diffusive protons is analytically derived.

In this paper, we improve the accumulative diffusion model by incorporating finite-volume of MCs (Sec. 2) and apply it to a series of interacting SNRs to reproduce the GeV-TeV spectra as well as the “platform” below the break at around GeV (Sec. 3).

## 2 ACCUMULATIVE DIFFUSION MODEL WITH FINITE-VOLUME MCS

### 2.1 Model description

In Paper I, the distribution function, at an arbitrary point (at radius  $R_c$ ), of the energetic protons that escape from the spherical shock front (at radius  $R_s$ ) throughout the history of the SNR expansion is given by

$$f_{\text{cum}}(E_p, R_c, t_{\text{age}}) = \int_0^{t_{\text{age}}} \int_0^{2\pi} \int_0^\pi f(E_p, R(R_c, t_i, \theta, \phi), t_{\text{dif}}) R_s^2(t_i) \sin \theta d\theta d\phi dt_i, \quad (1)$$

where  $t_{\text{age}}$  is the age of the SNR,  $t_i$  the time at which the proton escapes from SNR surface,  $t_{\text{dif}}$  the diffusion time after escape ( $t_{\text{dif}} = t_{\text{age}} - t_i$ ), and  $f(E_p, R(R_c, t_i, \theta, \phi), t_{\text{dif}})$  the distribution function, at point C, of the energetic protons that escape from unit area at an arbitrary source point S on the spherical shock front surface (see Paper I for relevant notations). The diffusion coefficient is assumed to be in the form of  $D(E_p) = 10^{28} \chi (E_p/10\text{GeV})^\delta \text{cm}^2\text{s}^{-1}$ , where  $\chi$  is the correction factor of slow diffusion around the SNR (Fujita et al. 2009) and  $\delta$  is the energy dependent index of diffusion coefficient. The distance between the SNR and MC does not need to be larger than the size of SNR, namely condition  $R_c \gg R_s$  is not required as opposed to the point source injection models.

Following the treatment of the dynamical evolution of SNR in Paper I, we use the Sedov-Taylor law  $R_s = (2.026 E_{\text{SNR}} t^2 / \rho_0)^{1/5}$  for the adiabatic phase, where  $\rho_0 = 1.4 m_{\text{H}} n_0$  is the density of the interstellar (intercloud) medium, and  $R_s = (147 \epsilon E_{\text{SNR}} R_t^2 t^2 / 4\pi \rho_0)^{1/7}$  for the radiative phase, where  $R_t$  is the transition radius from the Sedov phase to the radiative phase,  $E_{\text{SNR}}$  is the supernova explosion energy, and  $\epsilon$  is a factor equal to 0.24 (Blinnikov et al. 1982; see also Lozinskaya 1992).

In Paper I, we assume that all the MC mass is concentrated in a point. Here we take the finite-volume of cloud into account and in order to describe the problem with spherical coordinates, we approximate it as a truncated cone which

subtends solid angle  $\Omega$  at the SNR center and has a thickness  $\Delta R_c$ . By averaging the distribution function  $f_{\text{cum}}$  (Eq. (1)) over the finite-volume, we obtain the mean distribution of the energetic protons in the MC at  $t_{\text{age}}$  as a function of  $E_p$

$$F_{\text{ave}}(E_p, t_{\text{age}}) = \frac{\int_{R_c - \Delta R_c/2}^{R_c + \Delta R_c/2} r^2 dr \int_0^{t_{\text{age}}} \int_0^{2\pi} \int_0^\pi f(E_p, R(r, t_i, \theta, \phi), t_{\text{dif}}) R_s^2 \sin \theta d\theta d\phi dt_i}{\int_{R_c - \Delta R_c/2}^{R_c + \Delta R_c/2} r^2 dr}. \quad (2)$$

In particular, for  $\Omega = 4\pi$ , we have the case that the SNR is enclosed by a molecular shell (as also assumed in Ohira et al. 2011).

In the calculation of the  $\gamma$ -rays from the nearby MC (of mass  $M_c$ ) due to p-p interaction, we use the analytic photon emissivity  $dN_\gamma/dE_\gamma$  developed by Kelner et al. (2006; also see Paper I). The gained photon energy is generally 10% of the energetic proton energy (e.g. Katz & Waxman 2008).

### 2.2 Model Performance

We now explore the model parameters and show how the spectra of escaping protons depends on the parameters. In the model described above, for a certain SNR, the model parameters are of two sorts: particle diffusion ( $p$ ,  $\delta$ ,  $\chi$ ) and MCs ( $R_c$ ,  $\Delta R_c$ ).

Figure 1 shows the dependence of the spectral shape of the energetic protons in the finite cloud volume on each parameter with other parameters fixed. Here we assume a middle-aged SNR with  $R_{\text{SNR}} = 20\text{pc}$ ,  $t = 27000\text{yr}$ ,  $n_0 = 1\text{cm}^{-3}$ , and  $E_{\text{SNR}} = 10^{51}\text{erg}$  and a proton illuminated MC at  $R_c = 25\text{pc}$ .

The spectral dependence on the MC thickness  $\Delta R_c$  is presented in Figure 1a, where we adopt  $\chi = 0.01$ ,  $p = 2.2$ , and  $\delta = 0.5$ . We plot three curves for different thicknesses:  $\Delta R_c \rightarrow 0$ ,  $\Delta R_c = 8\text{pc}$ , and  $\Delta R_c = 10\text{pc}$ . In the  $\Delta R_c \rightarrow 0$  case, the cloud volume is not considered, similar to the treatment in Paper I. We see that there are spectral breaks in the diffusive protons and find that, with the thickness increased, the slope change around the break becomes gentle and a “platform”-like pattern appears and gets broadened. This pattern is formed by the combination of particle distribution at different diffusion distances (within the cloud thickness), as the spectral peak shifts to higher energies with the increase of distance. The  $\Delta R_c = 10\text{pc}$  case represents the situation that the MC is in contact with the SNR shock surface ( $R_c = R_s + \Delta R_c/2$ ; such case is called ‘contact’ case hereafter), in which the proton spectrum does not show a low-energy cutoff/turn-over since some of the low-energy protons can diffuse into the cloud.

The spectral dependence on the escaping protons energy index  $p$  is given in Figure 1b, with parameters  $\chi = 0.01$ ,  $\Delta R_c = 15\text{pc}$ , and  $\delta = 0.5$  used. Three values of  $p$  are used for comparison:  $p = 1.8$  is the particle spectral index predicted by the DSA mechanism considering non-linear effects,  $p = 2$  is the typical index of Fermi-type accelerated particles, and  $p = 2.2$  is the source spectral index of the Galactic CRs derived from the diffusion model GALPROP (Strong et al. 2007). For the ‘contact’ case ( $\Delta R_c = 10\text{pc}$ ), it can be seen that the slopes (both below and above the break energy)

<sup>1</sup> Actually, our model in Paper I has been tested for the case that the SNR has a very small radius (e.g., for a very high ambient density), which can be approximated as a point-like source, and reproduced the results of the classical point-like continuous injection case using the same model parameters.

of the particle distribution increase with  $p$ . For the ‘non-contact’ case ( $R_c > R_s + \Delta R_c/2$ , e.g.  $\Delta R_c = 8$  pc), the slopes above the break are very similar to those of the ‘contact’ case, and the low energy cut-off becomes more prominent with the increase of  $p$ .

Figure 1c shows the spectral dependence on the diffusion coefficient index  $\delta$  (with  $\chi = 0.01$ ,  $\Delta R = 15$  pc, and  $p = 2.2$  fixed). The value of  $\delta$  is usually adopted in the range of 0.3–0.7 (Berezinskii et al. (1990)). Here we use three values of  $\delta$ :  $\delta = 0.3$ , very close to the Kolmogorov type diffusion index (0.33);  $\delta = 0.5$ , for the Kraichnan type diffusion; and  $\delta = 0.7$ . This parameter strongly influence the spectral pattern. The slope of the proton spectrum above the break conforms the relation  $\alpha_2 \sim p + \delta$  for the continuous point source injection case (Aharonian 2004). For the ‘contact’ case ( $\Delta R_c = 10$  pc), there exhibits a “platform” pattern extended to low energy, while for the ‘non-contact’ case ( $\Delta R_c = 8$  pc), the low energy cut-off becomes more significant with the increase of  $\delta$ .

As shown in Figure 1d, different correction factor of diffusion coefficient  $\chi$  gives different flux and width of the “platform”. With the increase of the  $\chi$  value, the number of the low energy protons increases and the number of the high energy protons decreases, namely, the particle distribution gets softened. This is because faster diffusing high energy protons diffuse into farther distance and the low energy ones become dominant at the concerned distance. Meanwhile, the width of “platform” becomes narrower and the slope of the proton spectra above the break energy keeps unchanged.

### 3 APPLICATION TO INDIVIDUAL SNRS

Extended GeV emission associated with interacting SNRs has recently been revealed by a series of Fermi-LAT observations (Abdo et al. 2009, 2010a,b,c,d; Castro & Slane 2010), some of which are also spatially resolved by the H.E.S.S. TeV observations. These SNRs form a special interesting class, which may be beneficial to unveil the enigma of the origin of the Galactic CRs. One of the most conspicuous features of such a class is the commonly present, often gentle, spectral break at around 1-10 GeV, which is difficult to be reproduced by leptons via inverse Compton emission (e.g. Abdo et al. 2010a). In addition, the TeV spectra are mostly steep, with the photon indices sometimes as high as  $\sim 3.0$ , which is also hard to be explained by the primary accelerated protons, but can be done by the proton diffusion scenario (e.g. Aharonian & Atoyan 1996; Torres et al. 2008; paper I; Ohira et al. 2011). Here we apply our improved accumulative diffusion model to the nine SNRs currently available of the class (W28, W41, W44, W49B, W51C, Cygnus Loop, IC443, CTB 37A, and G349.7+0.2) and reproduce the GeV-TeV spectral patterns as aforesaid.

The basic parameters of each SNR studied here are listed in Table 1 with  $E_{\text{SNR}} = 10^{51}$  erg and  $\eta = 10\%$  assumed. Since they are all interacting SNRs, we only consider the MC which is in touch with the shock surface (i.e., the ‘contact’ case, although in some cases not all the  $\gamma$ -rays is coming from a contact MC). Thus we adopt the value of the lower-limit of the integration of Eq. (2) just the same as the value of the current shock radius, i.e.,  $R_c - \Delta R_c/2 = R_s$ .

In the  $\gamma$ -ray spectral fit, the parameters are adjusted

in the following way. Given a certain cloud mass (chiefly adopted from observation), the  $\gamma$ -ray flux can be roughly determined by changing the diffusion correction factor  $\chi$  (e.g., for point-like injection case,  $F_\gamma \propto \chi^{-3/2}$  (Gabici et al. 2010)). The broadness of the platform is fitted by adjusting the cloud thickness  $\Delta R_c$  for the fixed  $\chi$  and the slope of the “platform” and the slope above the break together with the TeV data can in turn be obtained with proper values of  $p$  and  $\delta$ .

#### 3.1 G6.4-0.1 (W28)

W28 is one of the prototype thermal composite (or mixed-morphology) SNRs, characterized by shell-like radio emission and centre-brightened thermal X-rays. It is an evolved SNR in the radiative phase, with an age estimate ranging from 35 to 150 kyr (Kaspi et al. 1993). In  $\gamma$ -rays the strongest TeV source is located at the northeastern edge of the remnant and positionally coincident with the well studied MC with which the remnant shock interacts (Aharonian et al. 2008a). In this  $\gamma$ -ray emitting region, there are some of the OH masers points detected in W28 (Frail et al. 1994). Recently, *Fermi* LAT observation found that the GeV source 1FGL J1801.3-2322c coincides with the TeV source and thus demonstrates a broken power-law for the  $\gamma$ -ray spectrum with a break at  $\sim 1$  GeV and photon indices of  $\sim 2.09$  below the break and  $\sim 2.74$  above the break (Abdo et al. 2010c). Three molecular clumps (Aharonian et al. 2008a) located outside the southern boundary of the remnant have different GeV and TeV brightness. In Paper I, we have explained the  $\gamma$ -ray spectra of the four sources via hadronic process of the diffusive protons, assuming different distances for the four sources. Here we also fit the spectrum of the northeastern source, taking the cloud volume into account. The result is very similar to that in Paper I. Unlike the sources in other SNRs studied in this paper, the “platform” below the break is unapparent (Figure 2(a)), entailing a large value of  $\chi$  and a small cloud thickness  $\Delta R_c$ . The evaluation of  $\chi$  also sensitively depends on the cloud mass.

#### 3.2 W41 (G23.3-0.3)

HESS J1834-087 used to be representative of a class of “dark”  $\gamma$ -ray sources, which was not thought to be firmly coincident with any detected sources (Aharonian et al. 2006). New H.E.S.S. analysis has revealed that the TeV emission can be divided into two components: the compact and extended ones. While the TeV compact component compatible with pulsar candidate does not seem to have GeV counterparts, the extended one, with index 2.7, may spatially match the GeV emission detected by *Fermi*-LAT from the SNR W41 region (Méhault et al. 2011), making this SNR a promising candidate for generating the observed extended  $\gamma$ -rays. The  $\gamma$ -ray spectrum in *Fermi* regime can be fitted by a single power-law with index 2.1, which causes a break between GeV and TeV.

This field is also observed in radio with VLA, CO, and X-rays with XMM-Newton. The high-resolution CO observation reveals its association with a giant molecular cloud with mass  $> 10^4 M_\odot$  (Tian et al. 2007). The strong absorption in X-rays together with the high the  $\gamma$ -ray to X-ray luminosity ratio ( $\sim 11$ ) indicates that the  $\gamma$ -rays may

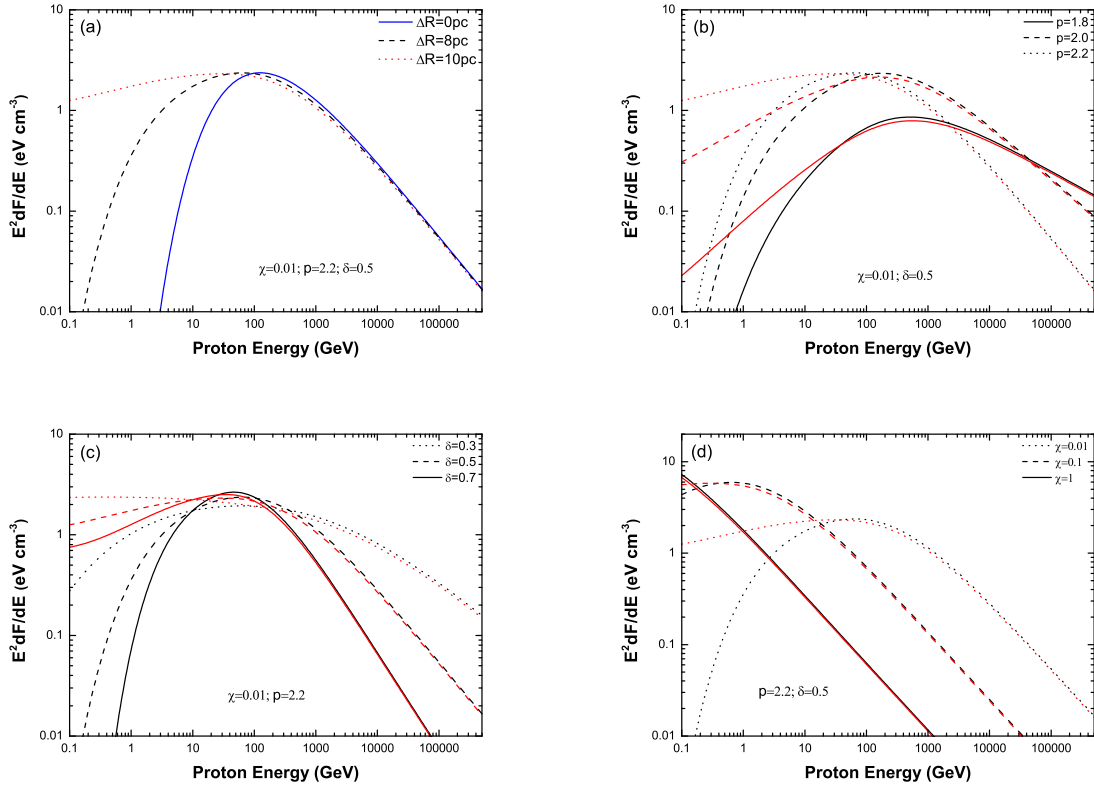


**Figure 1.** Spectra of the diffusive protons in the MCs for  $R_{\text{SNR}} = 20\text{pc}$ ,  $t = 27000\text{yr}$ ,  $n_0 = 1\text{cm}^{-3}$ ,  $E_{\text{SNR}} = 10^{51}\text{erg}$ , and  $R_c = 25\text{pc}$ . In panel (a),  $\Delta R_c = 0\text{pc}$  (blue),  $8\text{pc}$  (black), and  $10\text{pc}$  (red) are adopted, respectively. In panels (b)-(d), the black curves represent the case for  $\Delta R_c = 8\text{pc}$  and the red curves for  $\Delta R_c = 10\text{pc}$ .

**Table 1.** Dynamical evolution parameters for interacting SNRs

SNR	age(kyr)	distance(kpc)	angular size	$R_{\text{SNR}}(\text{pc})$	Reference
G6.4-0.1(W28)	42	1.9	48'	13.3	1, 2, 3
G23.3-0.3(W41)	100	4.2	33'	20.2	4
G34.7-0.4(W44)	20	2.8	30'	12.2	5,6
G43.3-0.2(W49B)	2	10	3'	4.4	7
G49.2-0.7(W51C)	30	6	30'	26.2	8,9
G74.0-8.5(Cygnus Loop)	20	0.54	180'	14.1	10,11,12
G189.1+3.0(IC443)	20	1.5	45'	9.8	6
G348.5+0.1(CTB 37A)	30	11.3	15'	24.7	13,14
G349.7+0.2	2.8	23	2'	6.7	14,15

References.-(1) Paper I; (2) Velázquez et al. 2002; (3) Green 2009; (4) Tian et al. 2007; (5) Abdo et al. 2010a; (6) Seta et al. 1998 (7) Brogan & Troland 2001; (8) Koo et al. 2005; (9) Moon & Koo 1997a; (10) Green 1990; (11) Blair et al. 2005; (12) Miyata et al. 1994; (13) Sezer et al. 2011; (14) Reynoso & Mangum 2000; (15) Slane et al. 2002

be of hadronic origin from energetic protons colliding with shocked GMC (Tian et al. 2007; Yamazaki et al. 2006).

The GeV “platform” of this source is the broadest ( $\sim 1-100\text{GeV}$ ) among the SNRs studied here (see Figure 2(b)). It thus requires a low diffusion coefficient ( $\chi \lesssim 10^{-2}$ ) and large thickness of cloud ( $\Delta R_c$  comparable to  $R_s$ ). With the parameters used (see Table 2), the well-determined TeV slope is also reproduced.

### 3.3 W44 (G34.7-0.4)

W44 is also a paradigm of “mixed-morphology” SNR, with semi-symmetric shape in radio with  $\sim 30'$  in size (Rho & Petre(1998)). It is considered to interact with a dense molecular cloud, with evidences including OH maser (Hoffman et al. 2005), molecular line broadening, CO line ratio (Castelletti et al. 2007), etc.

The  $\gamma$ -ray spectral energy distribution of W44 represents a broken power-law, which breaks at  $1.9\text{GeV}$ , with

**Table 2.** Fitted parameters for the  $\gamma$ -rays of interacting SNRs

SNR	$p$	$\delta$	$\chi$	$\Delta R(\text{pc})$	$M_{cl} (10^4 M_\odot)$
G6.4-0.1(W28)	2.2	0.5	0.05	0.5	5 <sup>a</sup>
G23.3-0.3(W41)	2.1	0.6	0.004	17	7 <sup>b</sup>
G34.7-0.4(W44)	2.4	0.7	0.02	7	3 <sup>c</sup>
G43.3-0.2(W49B)	2.4	0.6	0.03	3	1 <sup>d</sup>
G49.2-0.7(W51C)	2.2	0.5	0.04	7	1 <sup>e</sup>
G74.0-8.5(Cygnus Loop)	2.2	0.7	0.04	8	0.025 <sup>f</sup>
G189.1+3.0(IC443)	2.3	0.65	0.01	7	0.5 <sup>g</sup>
G348.5+0.1(CTB 37A)	2.1	0.6	0.02	5	5.8 <sup>h</sup>
G349.7+0.2	2.1	0.7	0.02	3	1.2 <sup>i</sup>

References.-(a) Aharonian et al. 2008a (b) Seta et al. 1998; (c) Seta et al. 2004; (d) Assumed; (e) Koo & Moon 1997 a,b; (f) Assumed (g) Cornett et al. 1977; (h) Reynoso & Mangum 2000; (i) Reynoso & Mangum 2001

photon indices 2.06 at low energy and 3.02 at high energy. Most of the  $\gamma$ -ray emission is inferred to arise from the SNR other than from the unresolved pulsar based on the resemblance between the  $\gamma$ -ray and infrared ring morphologies (Abdo et al. 2010a). Most recently, AGILE observation has also been reported with the  $\gamma$ -ray spectral down to 50 MeV. (Giuliani et al. 2011)

Figure 2(c) shows the fitting results of W44 using parameters listed in Table 2. Our fitting not only well reproduce the GeV “platform” spanned from 0.3 to 1.9 GeV, but also the spectrum with energy as low as 50 MeV, which is a robust advantage for hadronic origin of the  $\gamma$ -rays. It is noteworthy that the photon index above the break energy (3.02) is the largest among the 8 studied SNRs; we adopt the upper limit (0.7) of the usual range for  $\delta$  so as for  $p(=2.4)$  not to deviate too much from the common values (1.8-2.2). Although the VHE spectrum of W44 is the very steep, we predict that the flux around TeV energy is slightly higher than the H.E.S.S. detection limit and much higher than the expected sensitivity of new generation TeV telescope Cherenkov Telescope Array (CTA) (de Cea del Pozo et al. 2009).

### 3.4 W49B (G43.3-0.2)

W49B is a “mixed-morphology” SNR at a young age. Near-infrared shocked  $\text{H}_2$  emission suggests that W49B is an interacting SNR (Keohane et al. 2007). Particularly high abundances of hot Fe and Ni, and relatively metal-rich core and jet regions are interpreted as evidence that W49B is originated inside a wind-blown bubble inside a dense molecular cloud (Keohane et al. 2007).

Recently, *Fermi* LAT reported a GeV source spatially coincident with W49B (Abdo et al. 2010d). The spectrum, again, exhibits a broken power-law shape with break energy  $\sim 4.8\text{GeV}$  and the simple power-law can be rejected at a significance of  $4.4\sigma$ . More interestingly, the best-fit spatial position of the LAT source which seems coincident with the brightest part of the *Spitzer* IRAC  $5.8\mu\text{m}$  image strongly supports the scenario that the GeV emission is linked with the shocked gas. Recently, the H.E.S.S. collaboration has reported its detection in TeV and the photon spectrum is smoothly connected with GeV data points (Brun et al. 2010).

Due to the lack of definite value of the molecular mass

around this SNR, we assume  $M_{cl} \sim 10^4 M_\odot$  for fitting the  $\gamma$ -ray spectrum. The spectral slope below the break energy ( $< 4.8\text{GeV}$ ) is relatively large ( $\sim 2.2$ ) and, consequently, a large value of  $p (= 2.4)$  is inferred.

### 3.5 W51C (G49.2-0.7)

W51C is also a member of “mixed-morphology” type of SNRs. A partial shell  $\sim 30'$  in diameter with a breakout feature in northern part appears in the radio continuum (Moon & Koo 1994). A shock-MC interaction was shown by the observations of the shocked atomic and molecular gases (Koo & Moon 1997 a,b).

In the  $\gamma$ -rays, the H.E.S.S. collaboration has detected an extended VHE source coincident with W51C (Fiascon et al. 2009), and the Milagro observation reported a possible excess in this direction (Abdo et al. 2009). Recently, *Fermi* LAT detects the flux in this field and shows that the GeV spectrum has a “platform” below the break energy  $\sim 2\text{GeV}$  and cannot be described by a single power-law, which makes it difficult for leptonic models to reproduce the GeV spectrum (Abdo et al. 2009). Fang & Zhang (2010) explain the GeV-TeV spectrum with hadronic process, using the non-linear acceleration by low Mach number shock, and in this scenario the  $\gamma$ -rays arise from the acceleration region.

Considering the protons diffusion into the adjacent MC, we perfectly reproduce the GeV-TeV spectrum with typical parameters (e.g.,  $p = 2.2, \delta = 0.5$ ) as shown in Figure 2(e).

### 3.6 Cygnus Loop (G74.0-8.5)

The Cygnus Loop is one of the most famous and well-studied middle-aged SNRs. The  $\gamma$ -ray emission mapped by *Fermi*-LAT is along the SNR limb and appears to be broken into four parts, three of which are essentially in correspondence with  $\text{H}\alpha$  bright patches (Katagiri et al. 2011). Actually, there have been some evidence of the presence of dense gas along the SNR boundary. In the west, CO emission in  $-25$ – $+30 \text{ km s}^{-1}$  interval seems to be adjacent to the SNR (Dame 2001, see Katagiri et al. 2011) and two CO emission clumps at  $\sim +9.2 \text{ km s}^{-1}$  (with a mass  $\sim 100 M_\odot$ ) seems to be well in contact with the optical filament (Scoville et al. 1977). Shock excited near-IR  $\text{H}_2$  line emission associated with the SNR is detected from the northeastern boundary (Graham et al. 1991a,b). Also, according to the X-ray studies, dense

wall of cavity is suggested to be along the eastern edge (Levenson et al. 1997; Levenson, Graham & Snowden 1999) and shock-cloud interaction is thought to be taking place there (e.g., Miyata & Tsunemi 2001; Zhou et al. 2010). Such a molecular-rich environment may act as a reasonable site for the hadronic origin of  $\gamma$ -ray emission from shock accelerated CRs, which is pointed out by Katagiri et al. (2011).

*Fermi* LAT observation in the energy band 0.2–100 GeV shows a spectral break in the range 2–3 GeV. The  $\gamma$ -ray luminosity is  $\sim 1 \times 10^{33} \text{ erg s}^{-1}$ , which is lower than those of other GeV-emitting SNRs. The  $\gamma$ -ray spectrum can be reasonably fitted by our model. The fitting result is shown in Figure 2(f) with parameters listed in Table 2. To specify  $\Delta R_c$ , we adopt the inner and outer radii 0.7' and 1.6' of the  $\gamma$ -ray ring-like structure (Katagiri et al. 2011).

### 3.7 IC443 (G189.1+3.0)

IC 443 is one of the most thoroughly studied interacting SNRs, with rich evidence including the OH masers from the central and southeast regions (Hewitt et al. 2006), CO line ratio (Seta et al. 1998), molecular line broadening (Dickman et al. 1992), near-infrared shocked  $\text{H}_2$  emission (Rosado et al. 2007), etc.

In  $\gamma$ -rays, there are several sources coincident with IC 443 as observed by EGRET (Hartman et al. 1999), AGILE (Tavani et al. 2010), and *Fermi* (Abdo et al. 2010b) in GeV and MAGIC (Albert et al. 2007) and VERITAS (Acciari et al. 2009) in TeV. The spectrum can be represented by a broken power law with slopes of 1.93 and 2.56 and with a break at 3.25 GeV and show very broad “platform” below the break (Figure 2(f)).

The multi-band photon spectra, with only the EGRET data then available in GeV band, was explained by using a time-dependent model for non-thermal particles emitting in the acceleration region (Zhang & Fang 2008). Torres et al. used the point source diffusion model assuming two clouds (with volumes ignored) in the vicinity of IC443 to explain the GeV-TeV connection (Torres et al. 2010).

As shown in Figure 2(f), the  $\gamma$ -ray spectrum of IC443 is fitted assuming one cloud with geometric volume. The broad GeV “platform” is reproduced with a low diffusion coefficient ( $\chi \sim 10^{-2}$ ) and a large thickness of cloud required.

### 3.8 CTB 37A (G348.5+0.1)

SNR CTB 37A has a partial shell with a extended breakout to the south (Kassim et al. 1991). The 1720 MHz OH masers (Frail et al. 1996) and morphologically correspondent CO emission (Reynoso & Mangum 2000) demonstrate that this SNR is interacting with MCs.

In high energy  $\gamma$ -rays, H.E.S.S. has detected TeV emission in the field of CTB 37A. For the absence of X-ray synchrotron emission, it is unlikely that the leptonic scenario could explain these VHE emission and a hadronic origin would be favorable (Aharonian et al. 2008b). Recently, an unresolved source lies within the eastern shell of CTB 37A was detected by *Fermi* LAT, and the spectrum in *Fermi* regime, too, shows a “platform” below 4.2 GeV (Castro & Slane 2010). The GeV-TeV spectrum is well fitted (see Figure 2(g)) with parameters listed in Table 2.

### 3.9 G349.7+0.2

G349.7+0.2 is one of the radio and X-ray brightest SNRs in the Galaxy, with an blowout morphology (Slane et al. 2002). It has been shown to be an interacting SNR, with numerous evidences including the OH masers (Frail et al. 1996), CO line ratio of different transitions, molecular line broadening (Dubner et al. 2004), near-infrared(IR) shocked  $\text{H}_2$  emission (Reach et al. 2006), etc.

The *Fermi* LAT observation shows a bright  $\gamma$ -ray source in its field with a significance from the evaluation of the test statistic  $\sim 10\sigma$ . The spectrum exhibits a broken power law with break energy  $\sim 16\text{GeV}$  (Castro & Slane). As yet, no TeV excess has been reported in this direction. With the spectral fitting (see Figure 2(h)), we predict that the flux around TeV energy is slightly higher than the H.E.S.S. detection limit and much higher than the expected sensitivity of CTA.

## 4 DISCUSSION AND SUMMARY

In this paper, the accumulative diffusion model for CRs escaping from SNR shock (Paper I) is refined by considering the finite-volume clouds in the vicinity of SNRs. The variation of the proton spectra with different model parameters are also shown for exploring the parameter space. This refined model is applied to nine Galactic SNRs which are thought to be interacting with the ambient dense material, and their GeV spectral breaks/“platform”s, together with available TeV data, are naturally fitted.

For the four SNRs (W51C, W28, W44 and IC443), Ohira et al. (2011) obtain the momentum breaks of proton spectra and successfully explain the  $\gamma$ -ray spectral shapes. In our model, in addition to fitting the spectral shapes, the real differential fluxes in  $\gamma$ -rays are also calculated, with the cloud masses considered. For all nine SNRs, the parameter  $\delta$ , which gives the energy dependence of the diffusion coefficient, is used in an interval from 0.5 to 0.7, which is in the commonly favored range 0.3–0.7. The difference of the spectral fit parameters between our model and Ohira et al.’s (2011) ( $\delta = 0.19 - 0.62$ ) may be primarily caused by two factors. The first factor is the different assumption of escaping spectrum of protons: in their model, the time evolution of maximum energy and the delta-function momentum of the escaping protons are assumed, and in our model, typical power-law distribution for escaping protons is used (e.g., Aharonian & Atoyan 1996; Torres et al. 2008). The second factor is the relative positions between the shock and the  $\gamma$ -ray emitting MC: in their calculation, the MC is placed on the wall of stellar wind bubble separated from the shock (namely, the ‘non-contact’ case), while in our calculation, the ‘contact’ case is considered.

For fitting the GeV-TeV spectra of these interacting SNRs, the diffusion coefficients (see Table 2) are required to be much smaller ( $\chi \sim 10^{-2}$ ) than the averaged Galactic value  $\sim 1$  and are also different from the values used in Ohira et al. (2011), which are in a wide range from 0.01 to 1. Such small values of  $\chi$  have been noticed in observation by several authors (e.g., Fujita et al. 2009; Giuliani et al. 2010; Paper I; Gabici et al. 2010; Torres et al. 2011) when applying the proton diffusion to the  $\gamma$ -ray sources in the vicinity

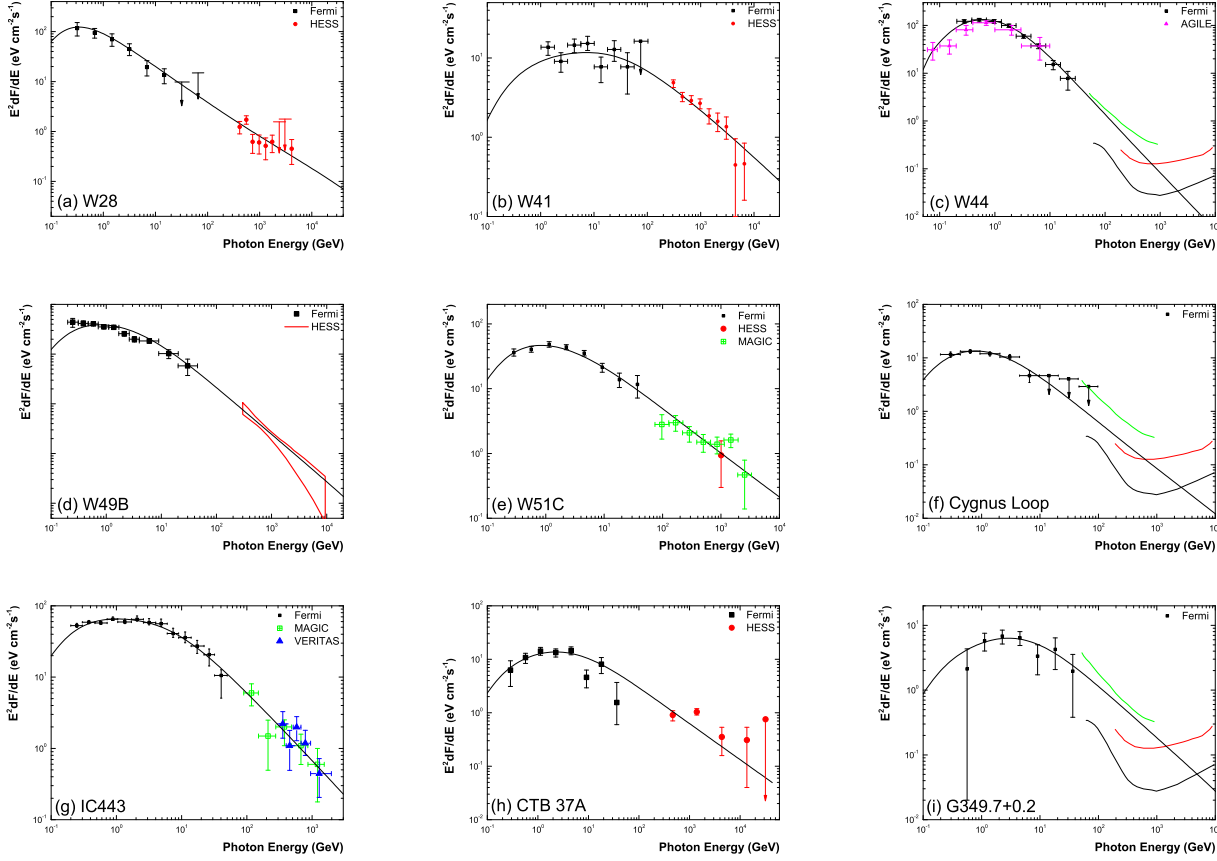


**Figure 2.**  $\gamma$ -ray spectral data of the eight interacting SNRs and the model spectra. The black square and red dot show the data points observed by *Fermi* and H.E.S.S., respectively. The sensitivity curves for MAGIC (green), H.E.S.S. (red), and CTA (black) are also shown in (c), (f) and (i). Panels from (a) to (h) represent the spectra fit of SNRs W28, W41, W44, W49B, W51C, Cygnus Loop, IC443, CTB 37A, and G349.7+0.2, respectively. (See text in Sec. 3)

of SNRs. Theoretically, this phenomenon is also studied by Monte-Carlo simulation, in which the CR streaming instability can generate Alfvén waves. The waves strongly scatter the particles and make the particle diffusion in the ISM around the SNR remarkably slow, and the diffusion coefficient is therefore strongly suppressed (Fujita et al. 2010; Fujita et al. 2011). This kind of suppression is significant if the ambient ISM is well ionized for the cosmic rays around the SNRs, because the neutral damping of Alfvén waves is not effective.

For small  $\chi$ , the typical diffusion velocity for certain particle energy may be smaller than the shock velocity, and the low energy cosmic rays will be continuously overrun by the SNR and reaccelerated. When considering particle acceleration, one needs a small Bohm diffusion coefficient ( $D_{\text{bohm}}$ ) to ensure particles to be proximate to the shock and repeatedly cross it efficiently. The reason why particles escape is that their diffusion coefficient in the ISM ( $D_{\text{esc}}$ ) is much larger than the one near the shock, namely  $D_{\text{esc}} \gg D_{\text{Bohm}}$ . In our paper, even if the diffusion coefficient is about two orders of magnitude smaller than the Galactic average, this condition is satisfied well. Even if some of the escaping particles will be overrun by the shock, these particles only fill a much smaller volume near the shock surface than the volume

of the particles diffusion region. Therefore, the probability of reacceleration process is quite small.

Our accumulative diffusion model proves successful in explaining the  $\gamma$ -rays from the nine interacting SNRs, which is again indicative of the contribution of the protons escaping from SNR shocks to the diffusive CRs. This model shows its advantage in treating the hadronic emission which arises from the clouds near the SNR shocks. As a matter of fact, if the distance between the SNR and MC is considerably large than the SNR size, our result will be similar to the point-like injection case.

## Acknowledgments

We thank the anonymous referee for valuable comments and Stefano Gabici for the helpful advice on diffusion coefficient. Y.C. acknowledges support from NSFC grants 10725312 and the 973 Program grant 2009CB824800.

## REFERENCES

- Abdo, A. A., et al. 2009, *ApJL*, 706, L1
- Abdo, A. A., et al. 2010a, *Science*, 327, 1103

- Abdo, A. A., et al. 2010b, *ApJ*, 712, 459
- Abdo, A. A., et al. 2010c, *ApJ*, 718, 348
- Abdo, A. A., et al. 2010d, *ApJ*, 722, 1303
- Acciari, V. A., et al. 2009, *ApJL*, 698, L133
- Aharonian, F. A., & Atoyan, A. M. 1996, *A&Ap*, 309, 917
- Aharonian, F. A. 2004, Very high energy cosmic gamma radiation : a crucial window on the extreme Universe, by F.A. Aharonian. River Edge, NJ: World Scientific Publishing, 2004,
- Aharonian, F., et al. 2006, *ApJ*, 636, 777
- Aharonian, F., et al. 2008a, *A&Ap*, 481, 401
- Aharonian, F., et al. 2008b, *A&Ap*, 490, 685
- Albert, J., et al. 2007, *ApJL*, 664, L87
- Berezinskii, V. S., Bulanov, S. V., Dogiel, V. A., & Ptuskin, V. S. 1990, Amsterdam: North-Holland, 1990, edited by Ginzburg, V.L.,
- Blandford, R., & Eichler, D. 1987, *PhR*, 154, 1
- Blinnikov, S. I., Imshennik, V. S., & Utrobin, V. P. 1982, *Soviet Astronomy Letters*, 8, 361
- Brogan, C. L., & Troland, T. H. 2001, *ApJ*, 550, 799
- Brun et al., for the H.E.S.S. collaboration, Proceedings of the 25th Texas Symposium on Relativistic Astrophysics (Heidelberg, Germany, 2010), to appear in Proceedings of Science
- Carmona, E., Krause, J., Reichardt, I., & for the Magic Collaboration 2011, arXiv:1110.0950
- Castelletti, G., Dubner, G., Brogan, C., & Kassim, N. E. 2007, *A&Ap*, 471, 537
- Castro, D., & Slane, P. 2010, *ApJ*, 717, 372
- Cornett, R. H., Chin, G., & Knapp, G. R. 1977, *A&Ap*, 54, 889
- de Cea del Pozo, E., Torres, D. F., & Rodriguez Marrero, A. Y. 2009, *ApJ*, 698, 1054
- Dickman, R. L., Snell, R. L., Ziurys, L. M., & Huang, Y.-L. 1992, *ApJ*, 400, 203
- Dubner, G., Giacani, E., Reynoso, E., & Parón, S. 2004, *A&Ap*, 426, 201
- Fang, J., & Zhang, L. 2010, *MNRAS*, 405, 462
- Fiason, A., Kosack, K., Skilton, J., Gallant, Y., Hinton, J., Pülhofer, G. 2008, American Institute of Physics Conference Series, 1085, 361
- Frail, D. A., Goss, W. M., & Slysh, V. I. 1994, *ApJL*, 424, L111
- Frail, D. A., Goss, W. M., Reynoso, E. M., Giacani, E. B., Green, A. J., & Otrupcek, R. 1996, *AJ*, 111, 1651
- Fujita, Y., Ohira, Y., Tanaka, S. J., & Takahara, F. 2009, *ApJL*, 707, L179
- Fujita, Y., Ohira, Y., & Takahara, F. 2010, *ApJL*, 712, L153
- Fujita, Y., Takahara, F., Ohira, Y., & Iwasaki, K. 2011, *MNRAS*, 415, 3434
- Gabici, S., Aharonian, F. A., & Casanova, S. 2009, *MNRAS*, 396, 1629
- Gabici, S., Casanova, S., Aharonian, F. A., & Rowell, G. 2010, SF2A-2010: Proceedings of the Annual meeting of the French Society of Astronomy and Astrophysics, 313
- Giuliani, A., et al. 2010, *A&Ap*, 516, L11
- Giuliani, A., Cardillo, M., Tavani, M., et al. 2011, *ApJL*, 742, L30
- Graham, J. R., Wright, G. S., Hester, J. J., & Longmore, A. J. 1991a, *AJ*, 101, 175
- Graham, J. R., Wright, G. S., & Geballe, T. R. 1991b, *ApJL*, 372, L21
- Green, D. A. 2009, Bulletin of the Astronomical Society of India, 37, 45
- Hartman, R. C., et al. 1999, *ApJS*, 123, 79
- Hewitt, J. W., Yusef-Zadeh, F., Wardle, M., Roberts, D. A., & Kassim, N. E. 2006, *ApJ*, 652, 1288
- Hewitt, J. W., Yusef-Zadeh, F., & Wardle, M. 2009, *ApJL*, 706, L270
- Hoffman, I. M., Goss, W. M., Brogan, C. L., & Claussen, M. J. 2005, *ApJ*, 627, 803
- Inoue, T., Yamazaki, R., & Inutsuka, S.-i. 2010, *ApJL*, 723, L108
- Jiang, B., Chen, Y., Wang, J., Su, Y., Zhou, X., Safi-Harb, S., & DeLaney, T. 2010, *ApJ*, 712, 1147
- Kaspi, V. M., Lyne, A. G., Manchester, R. N., Johnston, S., D’Amico, N., & Shemar, S. L. 1993, *ApJL*, 409, L57
- Kassim, N. E., Weiler, K. W., & Baum, S. A. 1991, *ApJ*, 374, 212
- Katagiri, H., et al. 2011, arXiv:1108.1833
- Katz, B., & Waxman, E. 2008, *JCAP*, 1, 18
- Kelner, S. R., Aharonian, F. A., & Bugayov, V. V. 2006, *PRvd*, 74, 034018
- Keohane, J. W., Reach, W. T., Rho, J., & Jarrett, T. H. 2007, *ApJ*, 654, 938
- Koo, B.-C., & Moon, D.-S. 1997a, *ApJ*, 475, 194
- Koo, B.-C., & Moon, D.-S. 1997b, *ApJ*, 485, 263
- Koo, B.-C., Lee, J.-J., Seward, F. D., & Moon, D.-S. 2005, *ApJ*, 633, 946
- Ku, W. H.-M., Kahn, S. M., Pisarski, R., & Long, K. S. 1984, *ApJ*, 278, 615
- Levenson, N. A., et al. 1997, *ApJ*, 484, 304
- Levenson, N. A., Graham, J. R., & Snowden, S. L. 1999, *ApJ*, 526, 874
- Li, H., & Chen, Y. 2010, *MNRAS*, 409, L35 (Paper I)
- Lozinskaya, T. A. 1992, New York: American Institute of Physics, 1992,
- Malkov, M. A., Diamond, P. H., & Sagdeev, R. Z. 2011, *Nature Communications*, 2,
- Méhault, J., Hofverberg, P., Renaudz, M., Cohen-Tanugi, J., Acero, F., Feinstein, F., Grondiny, M.-H., Lemoine-Goumard, M. 2011, talk in the Roma Fermi Symposium
- Miyata, E., & Tsunemi, H. 2001, *ApJ*, 552, 624
- Moon, D.-S., & Koo, B.-C. 1994, *Journal of Korean Astronomical Society*, 27, 81
- Ohira, Y., Murase, K., & Yamazaki, R. 2011, *MNRAS*, 410, 1577
- Reach, W. T., et al. 2006, *AJ*, 131, 1479
- Reynoso, E. M., & Mangum, J. G. 2000, *ApJ*, 545, 874
- Reynoso, E. M., & Mangum, J. G. 2001, *AJ*, 121, 347
- Rho, J., & Petre, R. 1998, *ApJL*, 503, L167
- Rosado, M., Arias, L., & Ambrocio-Cruz, P. 2007, *AJ*, 133, 89
- Scoville, N. Z., Irvine, W. M., Wannier, P. G., & Predmore, C. R. 1977, *ApJ*, 216, 320
- Seta, M., et al. 1998, *ApJ*, 505, 286
- Seta, M., Hasegawa, T., Sakamoto, S., Oka, T., Sawada, T., Inutsuka, S.-i., Koyama, H., & Hayashi, M. 2004, *AJ*, 127, 1098
- Sezer, A., Gök, F., Hudaverdi, M., & Ercan, E. N. 2011, arXiv:1107.1054
- Slane, P., Chen, Y., Lazendic, J. S., & Hughes, J. P. 2002, *ApJ*, 580, 904



- Strong, A. W., Moskalenko, I. V., & Ptuskin, V. S. 2007, Annual Review of Nuclear and Particle Science, 57, 285
- Tang, Y. Y., Fang, J., & Zhang, L. 2011, ApJ, 739, 11
- Tavani, M., et al. 2010, ApJL, 710, L151
- Tian, W. W., Li, Z., Leahy, D. A., & Wang, Q. D. 2007, ApJL, 657, L25
- Torres, D. F., Rodriguez Marrero, A. Y., & de Cea Del Pozo, E. 2008, MNRAS, 387, L59
- Torres, D. F., Marrero, A. Y. R., & de Cea Del Pozo, E. 2010, MNRAS, 408, 1257
- Torres, D. F., Li, H., Chen, Y., et al. 2011, arXiv:1107.3470
- Uchiyama, Y., Blandford, R. D., Funk, S., Tajima, H., & Tanaka, T. 2010, ApJL, 723, L122
- Velázquez, P. F., Dubner, G. M., Goss, W. M., & Green, A. J. 2002, AJ, 124, 2145
- Yamazaki, R., Kohri, K., Bamba, A., Yoshida, T., Tsuribe, T., & Takahara, F. 2006, MNRAS, 371, 1975
- Zhang, L., & Fang, J. 2008, ApJL, 675, L21
- Zhou, X., Bocchino, F., Miceli, M., Orlando, S., & Chen, Y. 2010, MNRAS, 406, 223

This paper has been typeset from a  $\text{\LaTeX}$  file prepared by the author.